CrossMark

ORIGINAL PAPER

Highly sensitive electrochemical sensor for the food toxicant Sudan I based on a glassy carbon electrode modified with reduced graphene oxide decorated with Ag-Cu nanoparticles

Youzhi Yao[1,2] · Yunchun Liu[1] · Zhousheng Yang[1]

Abstract The authors describe a method for room temperature preparation of reduced graphene oxide (rGO) decorated with Ag-Cu nanoparticles (NPs). The nanocomposite (Ag-CuNP/rGO) was characterized by scanning electron microscopy, energy dispersive X-ray spectroscopy, X-ray photoelectron spectroscopy and transmission electron microscopy. A glassy carbon electrode (GCE) modified with this nanocomposite dispersed is shown to be a viable electrode for determination of Sudan I (best at a working voltage of −112 mV vs. Ag/AgCl), with remarkably increased electrochemical response to Sudan I compared to that of a plain GCE. The calibration plot is linear in the 1.0 nM to 10 μM concentration range, with a 0.4 nM detection limit (at a signal-to-noise ratio of 3). The method was successfully applied to the determination of Sudan I in ketchup and chili powder.

Keywords Nanomaterial · Synergistic electron transfer · Amperometry · Trace determination

✉ Zhousheng Yang
yzhoushe@mail.ahnu.edu.cn

1 Anhui Key Laboratory of chemo-Biosensing, College of Chemistry and Materials Science, Anhui Normal University, Wuhu 241000, People's Republic of China

2 Wuhu Institute of Technology, Wuhu 241000, China

Introduction

Sudan I (1-phenylazo-2-naphthol), one of synthetic lipophilic azo dyes and the most frequently used Sudan dye, is widely used in fields of petroleum, engine oil, coloring hydrocarbon solvents, textile colorants and spirit varnishing [1–3]. Sudan I is considered to be a genotoxic carcinogen and is classified as a category 3 carcinogen by the International Agency for Research on Cancer [4, 5]. The Food and Drug Administration (FDA) and European Union also classified Sudan dyes as illegal food-additives associated health risks [6]. Nonetheless, they are still overdosed and utilized illegally in some daily foodstuffs because of its colorfastness and low cost, particularly in chilli, powders, relishes, seasonings, sausages, etc. [7, 8]. Consequently, monitoring Sudan I in foodstuffs is still required in a variety of natural agricultural products and processed foods, and effective, rapid, low-cost, reliable and practicable methods are in high demand. Various analytical methods have been widely developed for determination of Sudan I, such as UV-visible spectrometry [9], high performance liquid chromatography [10], paper spray mass spectrometry [11] and surface plasmon resonance [12]. Luo et al. applied rapid fluorescence assay for Sudan dyes. The sensing system based on polyethyleneimine-coated copper nanoclusters exhibits low detection limits for Sudan I-IV (65, 70, 45, and 50 nM, respectively). [13]. The electrochemical method has shown an increasing application for the detection of Sudan I containing electroactive groups (phenol and azo) in the field of food safety, such as Pt/carbon nanotubes (CNTs) [14], CNT/iron(III)/porphyrin [15] and Ag/graphene oxide [16] have been reported. Satisfactory results have been obtained with detection limits of 3 nM, 10 nM and 1140 nM, respectively. In practical

application, the detection limit is above 1.0 nM which cannot fit the real requirements for the trace detection of Sudan I. Therefore, decreasing the detection limit for Sudan I is still challenge and worthy of further investigation.

As an ideal support material for the metal nanoparticles, reduced graphene oxide (rGO) can be produced in large scale and low cost. rGO sheets possess an increased conductivity compared with GO sheets owing to the restoration of the conjugated network in the rGO sheets. The oxygen-containing functional groups on rGO render it with extremely high specific surface area, superior electronic conductivity, excellent mechanical strength and elasticity [17–19]. rGO is considered as a perfect two dimensional carbon support for developing highly efficient catalysts [20–23].

Noble metals such as Au, Ag, Pd, Pt, and Rh have been combined to generate bimetallic nanocomposites with tunable and enhanced properties. For example, Han et al. fabricated Pt-Au bimetallic nanoparticles with irregular shape [24]. The synthesis of bimetallic Pd-Au was studied in harsh experimental conditions by Takehiro et al. [25]. The synergistic structural, bifunctional mechanism and electronic effects of the different metals and heterogeneous interfaces, it can endow the surface and the interface with improved catalytic properties [26], which are superior to those of their pure counterparts [27, 28]. Up to now, many substitutions of noble metals with inexpensive metals (Cu, Fe, Co, Ni, etc.) have been extensively studied and they also have high catalytic activity [29, 30]. Effective, simple method for substitution preparation and good performance still remains a challenging task. Bimetallic nanocomposite to act as an electrochemical sensing interface is being actively pursued by investigators [31, 32]. Copper has similar properties to gold and silver, whereas it is much less noble than Ag and Au [13]. Considering that the standard electrode potential of Cu^{2+}/Cu was relatively low, the copper nanoparticles were often easily oxidized and unstable. Ag nanoparticles have high electrical conductivity and oxidation stability [33], the addition of silver can prevent from the oxidation of the copper and increase its stability [34].

Ag-CuNP/rGO nanocomposite is rapidly synthesized through an effective method with the use of sodium borohydride ($NaBH_4$) as reducing agent at room temperature. Then, the electrochemical behavior of Sudan I on Ag-CuNP/rGO modified GCE was explored. Several factors affecting the electrochemical performances of the proposed sensor were also further optimized, including the Ag-CuNP/rGO amount, pH value and scan rate. Ag-CuNP/rGO modified electrode exhibited excellent electrochemical performance with extended linear ranges and low detection limit for Sudan I. Ag-CuNP/rGO/GCE was successfully used for the determination of Sudan I in ketchup and chili powder samples and validated with

High Performance Liquid Chromatography-Ultraviolet ray (HPLC–UV) method.

The fabrication process of Ag-CuNP/rGO-based sensor for the determination of Sudan I is shown in Scheme 1.

Experimental

Reagents and instrument

All reagents were purchased from Shanghai Chemical Reagent Company (http://www.reagent.com.cn) except Sudan I was purchased from Aladdin. All the chemicals were of analytical grade and used as received without further purification. Sudan I dissolved in ethanol was prepared into different concentration solutions, and stored at 4 °C in the dark. Phosphate buffer (0.10 M) with pH values from 5.0 to 8.0 was prepared with Na_2HPO_4 and NaH_2PO_4. All solutions were prepared with doubly distilled water.

Scanning electron microscopy (SEM) was performed on S-4800 field emission scanning electron microanalyses (Hitachi, Japan). X-ray photoelectron spectroscopy (XPS, Thermo ESCACLB 250) was used in surface chemical state analysis. Three kinds of prepared sample powder each were taken a small amount and dispersed in ethanol to form uniform suspensions, which were dropped on a copper grid for the transmission electron microscopy (TEM, JEOL-2010 with 200 kV accelerating voltage) analysis.

Electrochemical experiments were performed with a CHI660D electrochemical analyzer (Shanghai Chenhua Apparatus, China) with conventional three-electrode cells. The working electrode was a glassy carbon electrode (Φ = 3 mm) (GCE) modified Ag-CuNP/rGO (Ag-CuNP/rGO/GCE). The reference electrode was an Ag/AgCl (saturated KCl) electrode and platinum electrode was used as the auxiliary electrode. Prior to each experiment, solutions were purged with purified nitrogen for 15 min to remove oxygen. All the measurements were performed at room temperature unless otherwise specified.

Synthesis of Ag-CuNP/rGO nanocomposite

Graphene oxide (GO) was prepared from purified natural graphite by a modified Hummers method [35]. $NaBH_4$ was used as the reducing agent, which can be used to simultaneously reduce metal ions and GO [31]. Ag-CuNP/rGO nanocomposite was prepared according to the following procedures. In brief, sodium citrate (100 μl, 0.10 M) as an anticoagulant was added into 40 mL of GO water solution (2 mg mL^{-1}), then aqueous solutions of $CuSO_4$ (100 μL, 0.1 M) was added. The mixture was stirred for 30 min to complete the ion

Scheme 1 Schematic illustration of the fabrication process of Ag-CuNP/rGO nanocomposite-based sensor for the determination of Sudan I
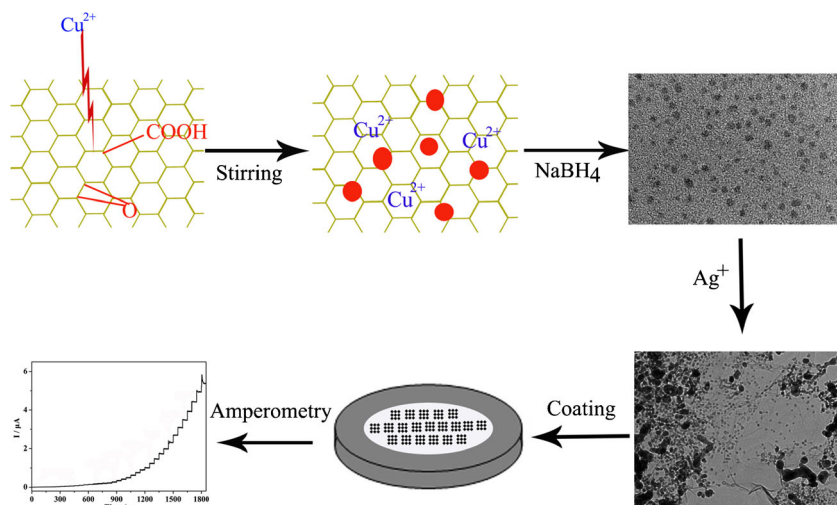
exchange and form Cu²⁺@GO complex due to functional groups on GO surface. Afterward, 3 mL of freshly prepared NaBH₄ (0.05 M) was added drop by drop into the mixture to reduce Cu²⁺ to Cu. About 15 min later, aqueous AgNO₃ solution (100 μL, 0.10 M) was added dropwise, and silver ions were reduced by residual reducing agent. The solution was stirred for 1 h, and the black solution was then left for settling for 24 h, upon which a black deposit was seen at the bottom. Remove the supernatant, the rest of the solution was processed by centrifugation (CT14D, 20,000 g, Shanghai, China.) at 10,000 rpm for 8 min and rinsed several times with deionized water and ethanol to remove all excess NaBH₄. The solid product was dried for 24 h in a vacuum oven at 25 °C and black powder was obtained. All the steps were carried out at room temperature.

Fabrication of the modified electrode

Prior to the modification, the GCE was polished to a mirror-like surface with 0.05 μm α-Al₂O₃, thoroughly rinsed with water and sonicated in absolute ethanol and water (each for 5 min). The three-electrode cell constructed of a platinum wire counter electrode, a saturated calomel electrode reference electrode and a working electrode prepared as following procedures: Ag-CuNP/rGO (1.0 mg) were dispersed into ethanol (9.50 mL). In order to fix modified electrode, nafion solution (0.50 mL) was also added in mixed liquid. After ultrasonication for 30 min to obtain a uniform suspension, the working electrode was prepared by placing 6 μL of the prepared suspension on a polished glass carbon electrode (GCE) and then drying the electrode at room temperature to form Ag-CuNP/rGO/GCE. For comparison, the rGO/GCE was also fabricated as the same procedure.

Results and discussion

Characterization

Morphology of Ag-CuNP/rGO nanocomposite

The morphologies of rGO and Ag-CuNP/rGO nanocomposite were examined by transmission electron microscopy (TEM) (Fig. 1). It is observed from (Fig. 1a) that a transparent and thin layer structure with some wrinkles and folds on the surface and edges is observed, which are the feature structure of graphene nanosheets. The TEM image of Ag-CuNP/rGO film (Fig. 1b) clearly shows the successful formation of Ag-CuNP/ rGO, a large number of Ag-Cu NPs were formed through the reduction of CuSO₄ and AgNO₃ by NaBH₄ and scattered on the rGO sheets, which would provide tremendous active sites for electrocatalysis. The high-resolution TEM (HRTEM) image of Ag/rGO nanocomposite gives the crystalline lattice fringes (Fig. 1c). Interlayer spacing of Ag was measured to be 0.238 and 0.196 nm, which can be assigned to the lattice spacing of (111) and (200) planes of fcc Ag, interlayer spacing of Cu (111) is 0.224 nm [36]. Ag-Cu NPs embedded into the rGO surface, indicating that Ag-Cu NPs were well bound to rGO sheets via chemical reduction. At the same time, the EDX spectrum of Ag-CuNP/rGO nanocomposite is shown in Fig. 1d, which confirms the presence of Ag and Cu elements. Contents of Ag and Cu are 48.96 and 28.46 wt%, respectively. Exhibited additional weak peak of oxygen element and other intense peaks were attributed to the silicon substrate.

Composition analysis of Ag-CuNP/rGO nanocomposite

The chemical composition analysis of Ag-CuNP/rGO nanocomposite was further characterized and compared with GO by XPS. The wide scan (corresponding to C1s, Ag3d and Cu2p) and C1s spectra of GO (I) and Ag-

Fig. 1 TEM images of rGO **a** and Ag-CuNP/rGO **b**; HRTEM image **c** and EDX **d** of Ag-CuNP/rGO
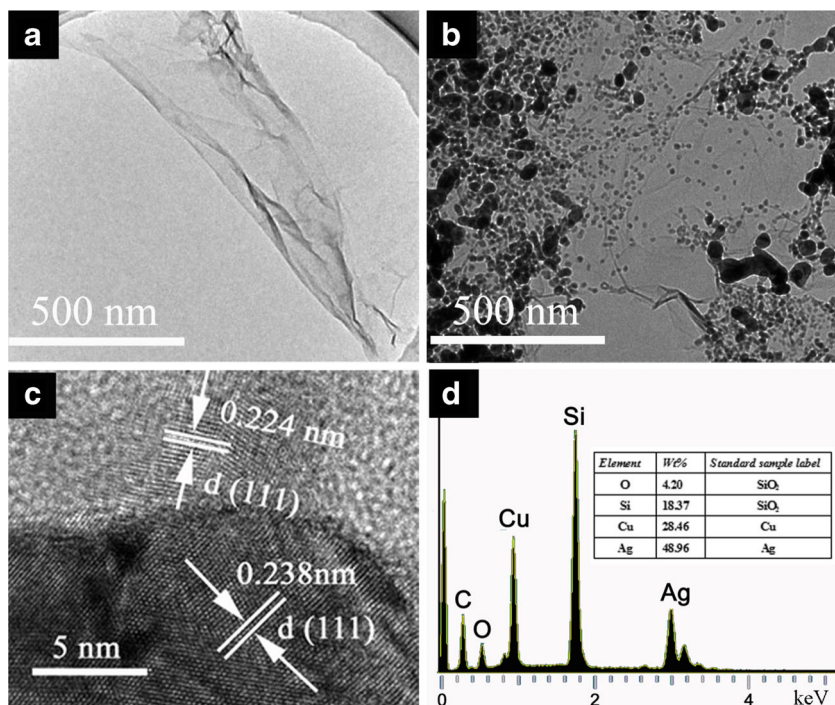
CuNP/rGO nanocomposite (II) are shown in Fig. 2a and b, Ag3d and Cu2p spectrums of Ag-CuNP/rGO are shown in Fig. 2c and d, respectively. It can be seen that the high-resolution C1s XPS spectrum of GO contains mainly three peaks positioned at approximately 284.6, 286.6 and 288.4 eV (Fig. 2b (I)), which is attributed to C-C (sp2 bonding in the GO), C-O (epoxy and acid groups) and C = O (carbonyl groups), respectively. After the GO is

Fig. 2 Wide scan XPS spectra **a** and C1s XPS spectra **b** of GO (I) and Ag-CuNP/rGO (II); Ag3d **c** and Cu2p **d** XPS spectrums of Ag-CuNP/rGO
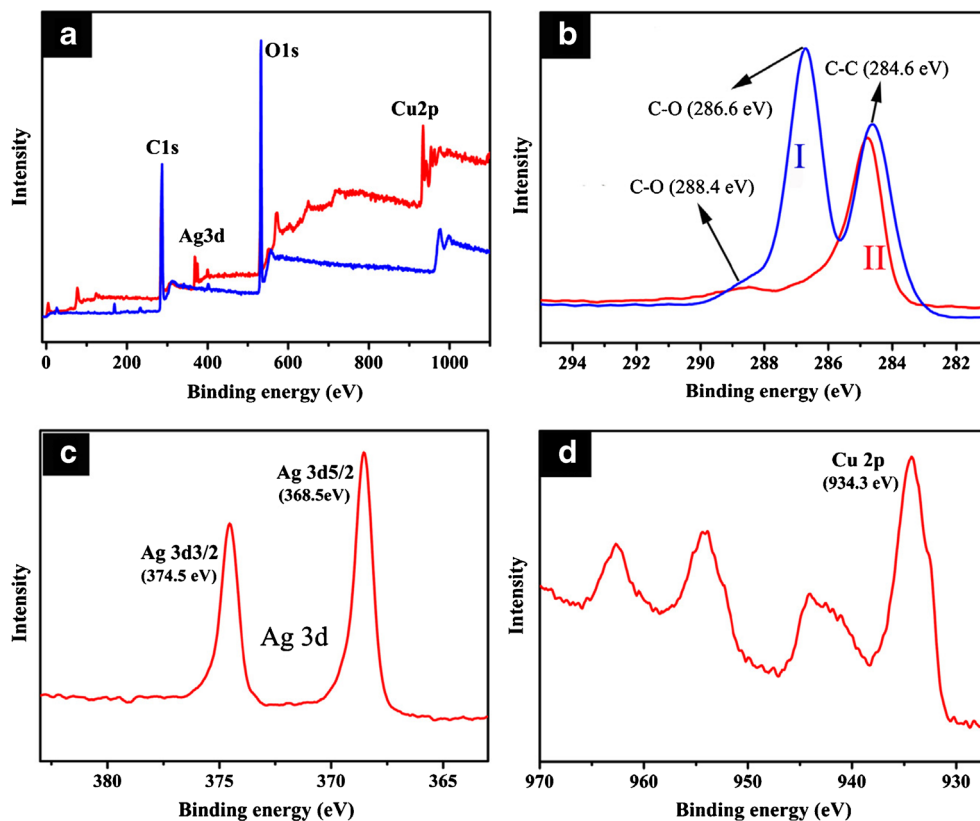
reduced, the corresponding XPS spectrum of Ag-CuNP/rGO (Fig. 2b (II)) shows that the intensities of C-O and C = O decrease dramatically, the peak associated with C-C becomes predominant, indicating that GO has been well deoxidized and formed rGO. The XPS patterns of Ag-CuNP/rGO nanocomposite in Fig. 2c and d represent the signatures of the Ag3d doublet (3d5/2 (368.5 eV) and 3d3/2 (374.5 eV)) and Cu2p (934.3 eV), which are consistent with the Ag^0 and Cu^0 states [37, 38]. The signatures of the Ag3d and Cu2p further confirm that silver and copper were decorated on rGO.

Electrochemical characterization of GCE, rGO/GCE and Ag-CuNP/rGO/GCE

Electrochemical impedance spectroscopy (EIS) was employed to characterize the surface features of the modified electrode using the redox probe 1.0 mM $[Fe(CN)_6]^{3-/4-}$ containing 0.10 M KCl, and the result is shown in Fig. 3. As well known, the typical impedance spectrum (Nyquist diagram) is generally divided into two parts. One is a semicircle in the high frequency region which has the relationship with the electron transfer resistance. The semicircle diameter of the high-frequency region is equivalent to the resistance of the charge transfer on the electrode surface (R_{et}). The other is a straight line in the low frequency region which is usually controlled by the diffusion process [39]. Figure 3 illustrates the EIS results (Nyquist plots) of bare GCE (a), rGO/GCE (b) and Ag-CuNP/rGO/GCE (c) in the frequency range from 10^5 to 0.001 Hz with the potential of 0.218 V and amplitude of 0.005 V. The Nyquist plot was fitted using the Randles equivalent circuit (insert of Fig. 3), which the diffusion and kinetic control parameters is taken into consideration. The semicircle diameter in the impedance spectrum is equal to Rct and the

value of Rct depends on the properties of the electrode/solution interface. At the bare GCE, a semicircle of about 220 Ω in diameter and an almost straight tail line is observed in the low frequency region, which is characteristic of a diffusion limiting step of the electrochemical process. The diameter of the high frequency semicircle is apparently reduced at rGO/GCE and the Rct value was 154 Ω. The decrease of Rct suggests that the immobilized rGO film can attract more $[Fe(CN)_6]^{3-/4-}$ to the modified electrode surface due to the increased surface area. While the rGO film decorated Ag-CuNP/rGO, the diameter of the high frequency semicircle is further reduced, and the Rct value is ca. 100 Ω. This result may be attributed to the good conductivity of Ag-Cu NPs, which can enhance the electron transfer rate. The impedance change of the modification process also indicates that rGO and Ag-CuNP/rGO have been successfully modified on the GCE surface.

Electrochemical behavior of Ag-CuNP/rGO/GCE towards Sudan I

The electrochemical activity and sensing performance of Sudan I on Ag-CuNP/rGO/GCE were evaluated by CV. Figure 4 displays CV curves of GCE, rGO/GCE and Ag-CuNP/rGO/GCE in 0.10 M phosphate buffer (pH 6.5) with 5 μμ Sudan I at a scan rate of 100 mV s^{-1}. There is no obvious redox peak at the bare electrode (Fig. 4a). Under the same conditions, a weak reduction peak is observed at rGO/GCE with a peak potential of ca. -0.153 V (Fig. 4b), which can be ascribed to the transformation of −N = N− to −NH − NH−. Whereas no corresponding oxidation peak can be observed in the reverse scan, implying the electro-reduction of Sudan I is an irreversible process. It is clear that the peak current recorded at Ag-CuNP/rGO/GCE is much higher
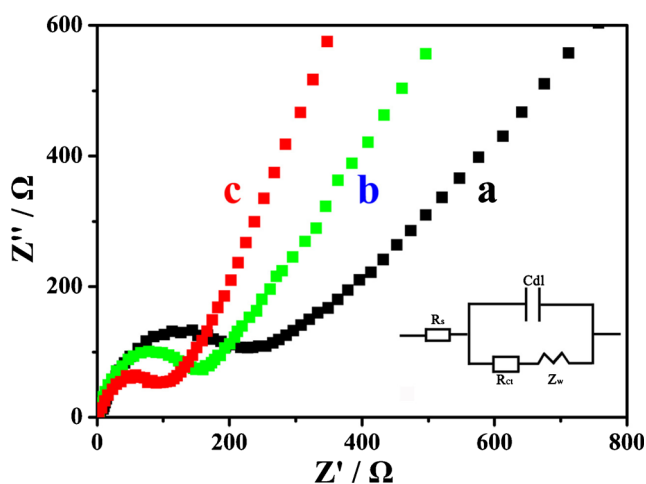

Fig. 3 Nyquist plots of different electrodes in 5.0 mM [Fe (CN)$_6$]$^{3-/4-}$ solution containing 0.10 M KCl. **a** bare GCE, **b** rGO/GCE and **d** Ag-CuNP/rGO
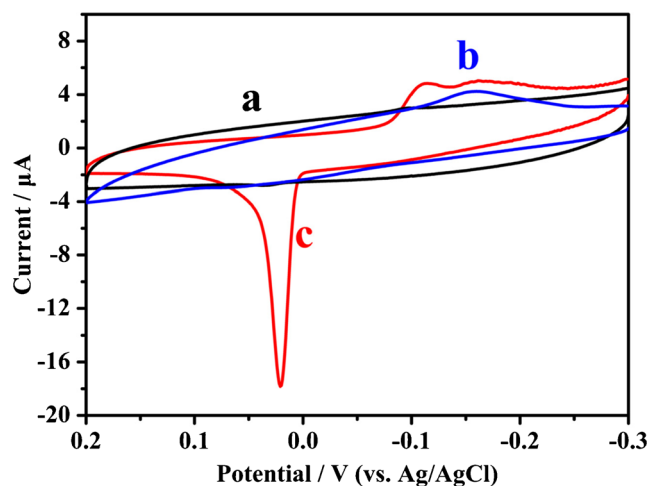

Fig. 4 Cyclic voltammograms of bare GCE **a**, rGO/GCE **b** and Ag-CuNP/rGO/GCE **c** in the presence of 5.0 × 10^3 nμ Sudan I in 0.10 M phosphate buffer (pH 6.5) at scan rate 100 mV s^{-1}

than that obtained at rGO/GCE (Fig. 4c). Another reduction peak is observed at Ag-CuNP/rGO/GCE with a peak potential of ca. -0.112 V, which may be due to the trans-

formation of $-NH-NH-$ to NH_2 group. Corresponding equation of electrochemical reaction for the Sudan I was shown below.
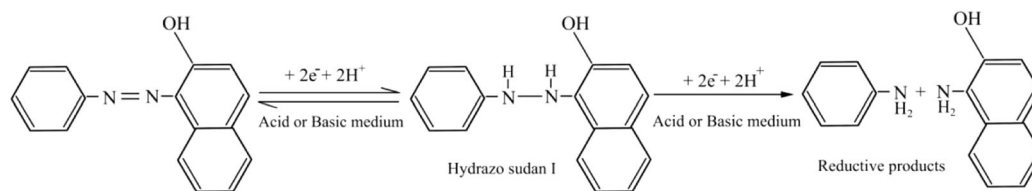
A sharp peak was observed with peak potential close to 0.022 V due to the oxidation of Ag atom [40], the peak potential of Sudan I shifted more positively to ca. -0.153 V. The electrochemical response of Sudan I on Cu/rGO/GCE displays larger peak current response compared with rGO/GCE and the electrochemical behavior of Sudan I on Ag/rGO/GCE emerges one reduction peak and Ag oxidation peak (Fig. S1, Electronic Supplementary Material, ESM). On the basis of these observations and comparisons, the doping of Ag-Cu NPs onto the rGO film displays excellent electrochemical activity towards Sudan I mainly due to the significant synergy effect. Intrinsic Ag surfaces have narrow d-band centers, when the metallic bond among the Ag atoms and Cu atoms were formed in the Ag-Cu NPs, the d-band centers of the Ag are broadened, which enhance catalytic activity [41]. Cu NPs existing in the rGO can also improve the absorption rate of Sudan I, increasing the concentration of the reactants and accelerating the electrochemical reaction process. Moreover, a large number of edge plane defect sites at the surface of Ag-CuNP/rGO may provide many favorable passageways for the electron transfer. According to the information, this electrochemical sensor can be used as an enhanced electrochemical performance for the sensitive detection of Sudan I.

Optimization of method

The following parameters were optimized: (a) Sample pH value; (b) Ag-Cu/rGO amount; (c) scan rate. Respective data and Figures are given in the Electronic Supporting Material (Fig. S2, Fig. S3, ESM). We found the following experimental conditions to give best results: (a) A sample pH value of 6.5; (b) Ag-Cu/rGO amount 6 µL (0.1 mg mL^{-1}); (c) the scan rate of 100 mV s^{-1} is performed.

Analytical performance

In order to develop a sensitively electrochemical sensor for the determination of Sudan I, the technique of amperometry was employed. Figure 5 shows the amperometric traces recorded

at Ag-CuNP/rGO/GCE at the applied potential −0.112 V, which Sudan I was spiked little by little every 50 s in phosphate buffer with continuous stirring under the optimal conditions. As shown in Fig. 5, good responses were observed
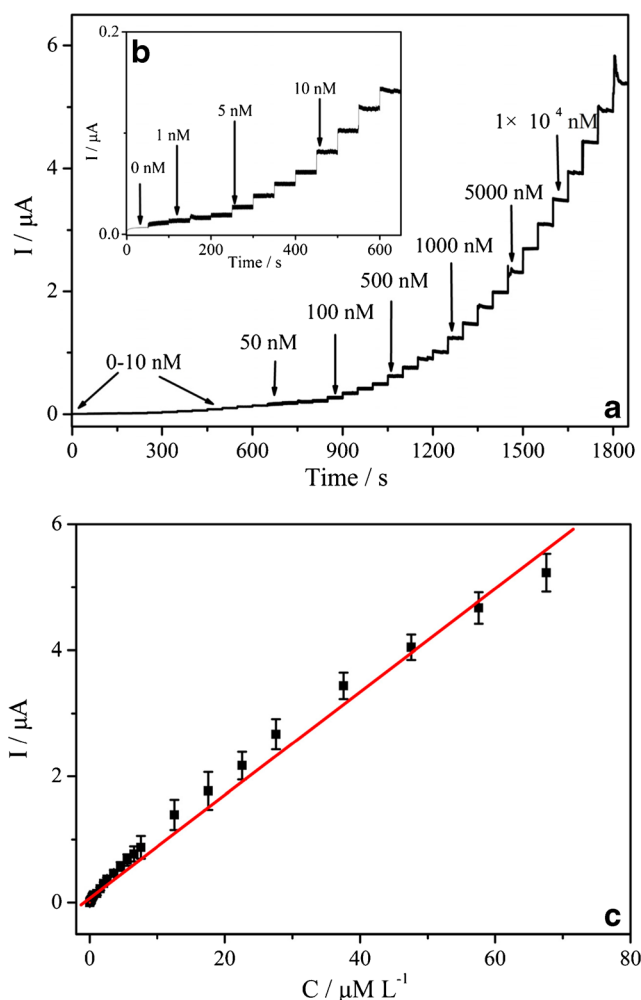

Fig. 5 Amperometric current-time curves for Sudan I reduction on the Ag-CuNP/rGO/GCE, applied potential at −0.112 V (versus Ag/AgCl) in phosphate buffer (pH 6.5): **a** the current-time curves for different concentrations of Sudan I, **b** the enlarged current-time curves for adding 0–10.0 nM of Sudan I, **c** the corresponding calibration curve

Table 1 Comparison of the method with other sensors for the determination of Sudan I

Electrode	Technique	Linear range (nM)	LOD (nM)	Reference
MWCNT[a]/GCE	SWV[b]	40.3–4030	20.1	42
MWCNT/GCE	Amperometry	1010–122,000	34.6	43
MIP[c]/AuNPs[d]/GCE	LSV[e]	100–10,000	2	44
Ag/graphene oxide/GCE	Amperometry	3900–31,900	1140	40
Electrochemically rGO/GCE	LSV	40–8000	10	45
MWCNT/chitosan/GCE	DPV	100–1000	30	46
CTAB-GNS[f]/GC	DPV	2–32,000	0.7	1
Ag–Cu/rGO/GCE	Amperometry	1–80,000	0.4	this work

[a] MWCNT: multiwalled carbon nanotube

[b] SWV: square wave voltammetry

[c] MIP: molecularly imprinting polymer

[d] AuNPs: goldnanoparticles

[e] LSV: Linear sweep voltammetry

[f] CTAB-GNS: Cetyl trimethyl ammonium bromide (CTAB) functionalized graphene nanosheets (GNS)

during the addition of Sudan I concentration from 1.0 nM to 1.0×10^4 nM. The response of preparing sensor to low-concentration Sudan I was shown in Fig. 5 (inset b), which demonstrated an effective catalytic property of Ag-CuNP/rGO material. The current was found to linearly increase with the Sudan I concentration in the range from 1.0 nM to 1.0×10^4 nM. The regression equation was Y (μA) = 0.1084 + 0.0818 C (μM) with the correlation coefficient being 0.995, and the detection limit was computed to be 0.4 nM (S/N = 3) at a signal-to-noise ratio of 3. The sensitivity was calculated as 7.36 μA mM^{-1}. The high sensitivity is attributed to the fact that high-density Ag and Cu nanoparticles increase the electrocatalytically active area. The two-dimensional structure of graphene which its large specific surface, in turn, supports the adsorption of Sudan I and electron transfer. In order to evaluate the analytical performance of the sensor, a literature comparison for Sudan I determinations using different modified electrodes is listed in Table 1 [1, 40, 42–46].

It can be found that Ag-CuNP/rGO/GCE provides a lowest detection limit among the electrodes described, and the linear range is wider than those obtained from most of other electrodes. The comparison suggests that the prepared nanocomposite in this work can be more appropriate to serve as a sensing platform for the sensitive determination of Sudan I in trace concentration.

Stability, reproducibility and selectivity of the sensor

The stability and reproducibility of Ag-CuNP/rGO/GCE were examined and the modified electrodes exhibited nice properties. When the Ag-CuNP/rGO/GCE was stored at room temperature for about 30 days, the peak currents of Sudan I decreased merely 3.7 %, indicating the high stability of Ag-CuNP/rGO/GCE. Under the optimized conditions, the

reproducibility of ten independently fabricated electrodes was investigated by comparing the peak currents of 500 nM Sudan I. The relative standard derivation (RSD) for the peak current is about 5.6 %. And the repeatability of one electrode was also detected by continuous measurements. The same sensor was used for approximately 15 times during three weeks and a small decrease of peak current (about 5.0 %) for Sudan I was observed.

The common potential interferents on the determination of Sudan I, especially some natural pigments, such as b-carotene, cryptoxanthin, lycopene and capsorubin, normally co-exist with Sudan I in real samples. These common potential interferents were individually examined under the optimized conditions. As shown in Fig. 6, with the addition of 500 nM Sudan I, peak current generated obvious change. Based on the tolerance limit of less than 5 % of the relative error for the
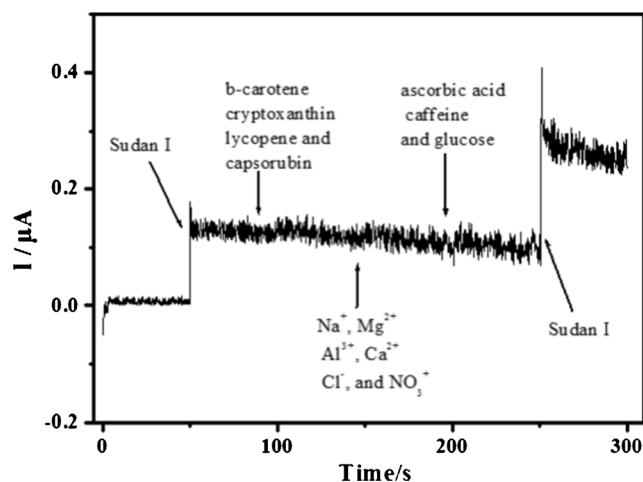

Fig. 6 Current-time responses obtained at the Ag-CuNP/rGO/GCE to 500 nM Sudan I and the interferents (indicated by arrows) in 0.10 M phosphate buffer (pH 6.5). Applied potential: −0.112 V

Table 2 Determination of Sudan I in real samples

Samples	Present method				HPLC–UV method		
	Added (nM)	Found (nM)	Recovery (%)	RSD (%)	Found (nM)	Recovery (%)	RSD (%)
Ketchup 1	200	196	98.0	3.6	193	96.5	4.2
Ketchup 2	300	293	97.7	2.9	286	95.3	3.2
Ketchup 3	400	405	101.2	4.2	392	98.0	4.9
Chilli sauce 1	200	209	104.5	4.7	205	102.5	5.3
Chilli sauce 2	300	291	97.0	3.9	287	95.7	4.8
Chilli sauce 3	400	389	97.2	3.5	406	101.5	5.1

current values at the peak potential of 500 nM Sudan I, some other potential interferents such as 500-fold concentration of Na^+, Mg^{2+}, Al^{3+}, Ca^{2+}, Cl^-, and NO^{3-} were added, no significant change in peak current was observed. 100-fold concentration of ascorbic acid, caffeine and glucose had also no interference on Sudan I determination. In the presence of the interferences mentioned above, the peak current still increased linearly after adding 500 nM Suand I again. These results indicate that the modified electrode is highly selective towards the determination of Sudan I. Thus, the present method has an excellent prospect for the further applications. Some pharmaceutical molecules, such as acamprosate, acarbose, acetrizoic acid etc., will be further explored in follow-on experiments.

Analytical application of the sensor

In order to evaluate the feasibility of the proposed method for the practical applications, Ag-CuNP/rGO/GCE was employed for the measurement of Sudan I in chilli powder and ketchup sauce. The real samples were obtained from a local bazaar and pretreated according to Wu's method. Since no Sudan I was detected in those samples, then the standard addition method was adopted and the total content of Sudan I was determined to calculate the recovery. The results were shown in Table 2, the RSD is below 5.0 % and the recoveries range between 97.0 % and 104.5 %. The recovery values obtained with the developed method are compared with that obtained using HPLC–UV method and they are found to be in agreement suggesting good validation of the method, indicating that our method has an excellent precision and is feasible and reliable for practical applications.

Conclusions

Synergistic combination of Ag-Cu nanoparticles and rGO caused enhancement of peak currents for Sudan I at Ag-CuNP/rGO/GCE. Electrochemical experiments have demonstrated that Ag-CuNP/rGO material could increase active surface area, high electrical conductivity leading to fast electron transfer rate of Sudan I on Ag-CuNP/rGO. Incorporation of Ag-Cu nanoparticles improved the stability of sensor response based on metallic bond among the Ag atoms and Cu atoms. The method was satisfactorily applied for ketchup and chili samples with excellent recoveries. We hope to extend the application of this sensor in other real samples.

Compliance with ethical standards The author(s) declare that they have no competing interests.

References

1. Mao Y, Fan Q, Li J, Yu L, Qu L (2014) A novel and green CTAB-functionalized graphene nanosheets electrochemical sensor for Sudan I determination. Sensors Actuators B Chem 203:759
2. Yu W, Liu Z, Li Q, Zhang H, Yu Y (2015) Determination of Sudan I–IV in candy using ionic liquid/anionic surfactant aqueous two-phase extraction coupled with high-performance liquid chromatography. Food Chem 173:815
3. Xu X, Tian X, Cai L, Xu Z, Lei H, Wang H, Sun Y (2014) Molecularly imprinted polymer based surface plasmon resonance sensors for detection of Sudan dyes. Anal Methods 6:3751
4. Stiborova M, Martinek V, Rydlova H, Hodek P, Frei E (2002) Sudan I is a potential carcinogen for humans: evidence for its metabolic activation and Detoxication by human recombinant cytochrome P450 1 A1 and liver Microsomes. Cancer Res 62:5678
5. Li JH, Feng HB, Li J, Feng YL, Zhang YQ, Jiang JB, Qian D (2015) Fabrication of gold nanoparticles-decorated reduced graphene oxide as a high performance electrochemical sensing platform for the detection of toxicant Sudan I. Electrochim Acta 167:226
6. Commission Decision 2003/460/EC of 20 June 2003 on emergency measures regarding hot chilli and hot chilli products (2003) Off J Eur Communities L154:114
7. Calbiani F, Careri M, Elviri L, Mangia A, Pistara L (2004) I. Zagnoni, development and in-house validation of a liquid chromatography–electrospray–tandem mass spectrometry method for the simultaneous determination of Sudan I, Sudan II, Sudan III and Sudan IV in hot chilli products. J Chromatogr A 1042:123
8. Hu XG, Fan YA, Zhang Y, Dai GM, Cai QL, Cao YJ, Guo CJ (2012) Molecularly imprinted polymer coated solid-phase

microextraction fiber prepared by surface reversible addition–fragmentation chain transfer polymerization for monitoring of Sudan dyes in chilli tomato sauce and chilli pepper samples. Anal Chim Acta 731:40

9. Alothman ZA, Unsal YE, Habila M, Shabaka A, Tuzen M, Soylak M (2012) Membrane filtration of Sudan orange G on a cellulose acetate membrane filter for separation–preconcentration and spectrophotometric determination in water, chili powder, chili sauce and tomato sauce samples. Food Chem Toxicol 50:2709

10. Piao C, Chen L (2012) Separation of Sudan dyes from chilli powder by magnetic molecularly imprinted polymer. J Chromatogr A 1268:185

11. Taverna D, Donna LD, Mazzotti F, Policicchio B, Sindona G (2013) High-throughput determination of Sudan azo-dyes within powdered chili pepper by paper spray mass spectrometry. J Mass Spectrom 48:544

12. Xu XY, Tian XG, Cai LG, Xu ZL, Lei HT, Wang H, Sun YM (2014) Molecularly imprinted polymer based surface plasmon resonance sensors for detection of Sudan dyes. Anal Methods 6:3751

13. Ling Y, Li JX, Qu F, Li NB, Luo HQ (2014) Rapid fluorescence assay for Sudan dyes using polyethyleneimine-coated copper nanoclusters. Microchim Acta 181:1069

14. Elyasi M, Khalilzadeh MA, Karimi-Maleh H (2013) High sensitive voltammetric sensor based on Pt/CNTs nanocomposite modified ionic liquid carbon paste electrode for determination of Sudan I in food samples. Food Chem 141:4311

15. Wu YH (2010) Electrocatalysis and sensitive determination of Sudan I at the single-walled carbon nanotubes and iron(III)-porphyrin modified glassy carbon electrodes. Food Chem 121:580

16. Prabakaran E, Pandian K (2015) Amperometric detection of Sudan I in red chili powder samples using Ag nanoparticles decorated graphene oxide modified glassy carbon electrode. Food Chem 166:198

17. Geim AK, Novoselov KS (2007) The rise of grapheme. Nat Mater 6:183

18. Sahoo NG, Pan YZ, Li L, Chan SH (2012) Graphene-based materials for energy conversion. Adv Mater 24:4203

19. Kong BS, Geng J, Jung HT (2009) Layer-by-layer assembly of graphene and gold nanoparticles by vacuum filtration and spontaneous reduction of gold ions. Chem Commun 16:2174

20. Yang L, Wang G, Liu Y (2013) An acetylcholinesterase biosensor based on platinum nanoparticles–carboxylic graphene–nafion-modified electrode for detection of pesticides. Anal Biochem 437:144–149

21. Gong J, Miao X, Zhou Z, Zhang L (2011) An enzymeless organophosphate pesticide sensor using Au nanoparticle-decorated graphene hybrid nanosheet as solid-phase extraction. Talanta 85:1344

22. Lu XQ, Qi HT, Zhang XF, Xue ZH, Jin J, Zhou XB, Liu XH (2011) Highly dispersive Ag nanoparticles on functionalized graphene for an excellent electrochemical sensor of nitroaromatic compounds. Chem Commun 47:12494

23. Luo J, Jiang SS, Zhang HY, Jiang JQ, Liu XY (2012) A novel non-enzymatic glucose sensor based on Cu nanoparticle modified graphene sheets electrode. Anal Chim Acta 709:47

24. Vilian ATE, Hwang SK, Kwak ChH OSY, Kim CY, Lee G, Lee Jin B, Huh YS, Han YK (2016) Pt-Au bimetallic nanoparticles decorated on reduced graphene oxide as an excellent electrocatalysts for methanol oxidation. Synth Met 219:52

25. Takehiro N, Liu P, Bergbreiter A, Nørskovb JK, Behm RJ (2014) Hydrogenadsorption on bimetallic Pd-Au(111) surface alloys: minimum adsorptionensemble, ligand and ensemble effects, and ensemble confinement. PhysChem Chem Phys 16:23930

26. Ding LX, Li GR, Wang ZL, Liu ZQ, Liu H, Tong YX (2012) Porous Ni@Pt Core-Shell nanotube Array Electrocatalyst with high activity and stability for methanol oxidation. Chem-Eur J 18:8386

27. Yin AX, Min XQ, Zhu W, Liu WC, Zhang YW, Yan CH (2012) Pt-Cu and Pt-Pd-Cu concave nanocubes with high-index facets and superiorelectrocatalytic activity. Chem Eur J 18:777–782

28. Yano H, Kataoka M, Yamashita H, Uchida H, Watanabe M (2007) Oxygenreduction activity of carbon-supported Pt-M (M = V, Ni, Cr, Co, and Fe) alloysprepared by nanocapsule method. Langmuir 23:6438

29. Mao H, Li RS, Jiang K, Huang T, Yu AS (2013) Facile preparation of Cu@Pt/rGO hybrids and their electrocatalyticactivities for methanol oxidation. Electrochim Acta 107:419

30. Sreedhar NY, Kumar MS, Krishnaveni K (2015) Sensitive determination of chlorpyrifos using Ag/Cu alloynanoparticles and graphene composite paste electrode. Sensors Actuators B 210:475

31. Li FH, Guo YQ, Liu Y, Qiu HX, Sun XY, Wang W, Liu Y, Gao JP (2013) Fabrication of Pt–Cu/RGO hybrids and their electrochemical performance for the oxidation of methanol and formic acid in acid media. Carbon 64:11

32. Mao H, Li RS, Jiang K, Huang T, Yu AS (2011) Facile preparation of Cu@Pt/rGO hybrids and their electrocatalytic activities for methanol oxidation. Electrochim Acta 107(2013):419–424

33. Osch THJ, Perelaer J, Laat AWM, Schubert US (2008) Inkjet printing of narrow conductive tracks on untreated polymeric substrates. Adv Mater 20:343

34. Li GP, Luo YJ (2008) Preparation and characterization of dendrimer-templated Ag–Cu bimetallic nanoclusters. Inorg Chem 47:360

35. Hummers JW, Offeman RE (1958) Preparation of graphitic oxide. J Am Chem Soc 80:1339

36. Kang P, Bobyr E, Dustman J, Hodgson KO, Hedman B, Solomon EI, Stack TDP (2010) Bis(μ-oxo) Dicopper(III) species of the simplest Peralkylated diamine: enhanced reactivity toward exogenous substrates. Inorg Chem 49:11030

37. Ma LB, Shen XP, Ji ZY, Zhu GX, Zhou H (2014) Ag nanoparticles decorated MnO2/reduced graphene oxide as advanced electrode materials for supercapacitors. Chem Eng J 252:95

38. Jia ZF, Chen TD, Wang J, Ni JJ, Li HY, Shao X (2015) Synthesis, characterization and tribological properties of Cu/reduced graphene oxide composites. Tribol Int 88:17

39. Li C, Liu W, Gu Y, Hao S, Yan X, Zhang Z, Yang M (2014) Simultaneous determination of catechol and hydroquinone based on poly (sulfosalicylic acid)/functionalized graphene modified electrode. J Appl Electrochem 44:1059

40. Prabakaran E, Pandian K (2015) Amperometric detection of Sudan I in red chili powder samples using Ag nanoparticles decorated graphene oxide modified glassy carbon electrode. Food Chem 166:198

41. Duan DH, Liu HH, You X, Wei HK, Liu SB (2015) Anodic behavior of carbon supported Cu@Ag core–shell nanocatalysts in direct borohydride fuel cells. J Power Sources 293:292

42. Gan T, Li K, Wu K (2008) Multi-wall carbon nanotube-based electrochemical sensor for sensitive determination of Sudan I. Sensors Actuators B Chem 132:134

43. Yang D, Zhu L, Jiang X (2010) Electrochemical reaction mechanism and determination of Sudan I at a multi wall carbon nanotubes modified glassy carbon electrode. J Electroanal Chem 640:17

44. Chen S, Du D, Huang J, Zhang A, Tu H, Zhang A (2011) Rational design and application of molecularly imprinted sol–gel polymer for the electrochemically selective and sensitive determination of Sudan I. Talanta 84:451

45. Zhang L, Zhang X, Li X, Peng Y, Shen H, Zhang Y (2013) Determination of Sudan I using electrochemically reduced graphene oxide. Anal Lett 46:923

46. Wu M, Tang W, Gu J, Wang Q, He P, Fang Y (2013) Electrochemical detection of Sudan I using a multi-walled carbon nanotube/chitosan composite modified glassy carbon electrode. Am J Anal Chem 4:1